

On the Design of Nonlinear MPC and LPVMPC for Obstacle Avoidance in Autonomous Driving*

Maryam Nezami¹, Dimitrios S. Karachalios¹, Georg Schildbach¹ and Hossam S. Abbas¹

Abstract—In this study, we are concerned with autonomous driving missions when a static obstacle blocks a given reference trajectory. To provide a realistic control design, we employ a model predictive control (MPC) utilizing nonlinear state-space dynamic models of a car with linear tire forces, allowing for optimal path planning and tracking to overtake the obstacle. We provide solutions with two different methodologies. Firstly, we solve a nonlinear MPC (NMPC) problem with a nonlinear optimization framework, capable of considering the nonlinear constraints. Secondly, by introducing scheduling signals, we embed the nonlinear dynamics in a linear parameter varying (LPV) representation with adaptive linear constraints for realizing the nonlinear constraints associated with the obstacle. Consequently, an LPVMPC optimization problem can be solved efficiently as a quadratic programming (QP) that constitutes the main novelty of this work. We test the two methods for a challenging obstacle avoidance task and provide qualitative comparisons. The LPVMPC shows a significant reduction in terms of the computational burden at the expense of a slight loss of performance.

I. INTRODUCTION

In recent years, there has been a growing interest in developing autonomous driving vehicles. One of the key challenges in autonomous driving is navigating through complex environments and avoiding collisions with obstacles safely. Model predictive control (MPC) is a powerful control algorithm that has been widely used in the area of autonomous driving. MPC is particularly effective in controlling a vehicle because it can incorporate prior knowledge of the system dynamics, environmental information, as well as state and input constraints when computing a control input. Considering these factors, MPC can generate optimized control inputs that satisfy the constraints, resulting in high system performance and safety.

MPC has been widely applied for obstacle avoidance in autonomous vehicles, see, e.g., [1]–[3]. It can be utilized to generate optimal trajectories that steer the vehicle away from obstacles in its path while respecting safety constraints. Given that vehicles are safety-critical systems, the use of nonlinear MPC (NMPC) is gaining popularity due to its ability to utilize high-fidelity nonlinear models of vehicle dynamics, thereby enabling more accurate and precise control actions. The work presented in [4] has objectives similar to the current study, but it assumed constant longitudinal speed to solve the NMPC problem with sequential quadratic

programs (SQP). In [5], an NMPC algorithm for path tracking has been proposed. This approach incorporates braking control before steering at high speeds. Investigating the effect of obstacle constraints on the algorithm’s performance is interesting. This paper aims to keep the vehicle’s operation stable while hard constraints are enforced in the optimization problem. In [6], a method for generating safe and efficient driving trajectories for autonomous vehicles using NMPC has been introduced. The numerical solution of the NMPC was obtained using a genetic algorithm strategy, which does not offer a guarantee of convergence.

The computational burden is a significant challenge for applying NMPC, particularly for systems with many states and constraints. Given the computational challenges, there has been increasing attention to linear parameter varying (LPV) modeling methods to embed nonlinear dynamics in a linear setting [7], [8]. Although the application of LPVMPC in autonomous driving has not yet received much attention in the literature, there are promising results reported in recent studies. In [9], a control architecture for lane-keeping has been suggested where a tube-based LPVMPC showed robust performance in lane-keeping. In [10], an online planning solution based on LPVMPC for autonomous racing has been proposed to improve the computational time while preserving the system’s performance.

Contributions: This paper proposes a novel LPV embedding for the nonlinear vehicle dynamics as a first step toward LPVMPC implementation. Such an LPV embedding could be of interest for convergence and feasibility analysis based on convex optimization tools. As a second step, at first, computation of the kinematic trajectories from a fixed map is presented. Then, we propose a linear formulation of the nonlinear constraints associated with the obstacle, which allows a tractable LPVMPC optimization problem using quadratic programming (QP). The proposed LPVMPC scheme integrates path planning and control into one optimization problem, deciding when to initiate the overtaking maneuver while ensuring the vehicle to be within the road boundaries. Finally, to verify the effectiveness of the proposed methods, simulation results are compared to the full nonlinear implementation, and further discussions are given.

Contents: Section II presents the nonlinear vehicle model and the nonlinear obstacle avoidance constraint, followed by the introduction of the linear representation of the obstacle constraint and the linear parameter varying modeling. In Section III, the models and constraints from Section II are used to set up the NMPC and the LPVMPC for obstacle avoidance. Section IV shows the implementation of the meth-

*D. S. Karachalios is funded by the Deutsche Forschungsgemeinschaft (DFG, German Research Foundation) - 419290163.

¹Institute for Electrical Engineering in Medicine, University of Lübeck, Lübeck, Germany {maryam.nezami, dimitrios.karachalios, georg.schildbach, h.abbas}@uni-luebeck.de

ods and compares their performance in the proposed obstacle avoidance scenarios. Finally, a few concluding remarks are presented in Section V.

Notations and definitions: The notation $Q \succ 0$ represents the positive definiteness of a matrix Q . The weighted norm $\|x\|_Q$ is defined as $\|x\|_Q^2 = x^T Q x$. The function $\text{diag}(x)$ constructs a diagonal matrix from a vector x . A halfspace is defined as $\{x \in \mathbb{R}^n | a^T x \leq b\}$. The set of positive integers, including zero, is denoted by $\mathbb{Z}_+ \cup \{0\}$.

II. VEHICLE MODEL AND CONSTRAINTS

Consider the following discrete-time nonlinear system

$$z_{k+1} = f(z_k, u_k), \quad \forall k \in \mathbb{Z}_+ \cup \{0\}, \quad (1)$$

where $z_k \in \mathbb{R}^n$ and $u_k \in \mathbb{R}^m$ are the state and input vectors, respectively, at the instant k . The initial condition is z_0 . The system is subject to the following state and input constraints:

$$z_k \in \mathcal{Z}_k \quad \text{and} \quad u_k \in \mathcal{U} = \{u_k \in \mathbb{R}^m | G^u u_k \leq h^u\}. \quad (2)$$

Here, \mathcal{Z}_k represents a time-varying set, and its formulation will be discussed in the subsequent section. Within the input constraint, we have $G^u \in \mathbb{R}^{q_u \times m}$ and $h^u \in \mathbb{R}^{q_u}$. The number of rows, q_u , depends on the number of inputs that have upper bounds, lower bounds, both upper and lower bounds, or no bounds at all. In this section, the representation of the vehicle dynamics in the form (1) using a dynamic bicycle model [11, p. 27] is given, as well as the constraints formulation to handle the obstacle avoidance.

A. Dynamic Bicycle Model

Based on [11, p. 27], the differential equations describing the motion at time $t \geq 0$ of a vehicle are presented as follows

$$\dot{X}(t) = v(t) \cos \psi(t) - \nu(t) \sin \psi(t), \quad (3a)$$

$$\dot{Y}(t) = v(t) \sin \psi(t) + \nu(t) \cos \psi(t), \quad (3b)$$

$$\dot{v}(t) = \omega(t)v(t) + a(t), \quad (3c)$$

$$\dot{\nu}(t) = -\omega(t)\nu(t) + \frac{2}{m}(F_{yf}(t) \cos \delta(t) + F_{yr}(t)), \quad (3d)$$

$$\dot{\psi}(t) = \omega, \quad (3e)$$

$$\dot{\omega}(t) = \frac{2}{I_z}(l_f F_{yf}(t) - l_r F_{yr}(t)), \quad (3f)$$

where X , Y , v , ν , ψ and ω denote the global X axis coordinate of the center of gravity (CoG), the global Y axis coordinate of the CoG, the longitudinal speed in body frame, the lateral speed in body frame, the vehicle yaw angle and the yaw angle rate, respectively. The control inputs of the system are the longitudinal acceleration a and the steering angle δ . The vehicle moment of inertia and mass are denoted by I_z and m , respectively. The lateral forces acting on the front and rear tires are denoted as F_{yf} and F_{yr} , respectively, and calculated as $F_{yf} = C_{\alpha f} \alpha_f$, $F_{yr} = C_{\alpha r} \alpha_r$. The parameters $C_{\alpha f}$ and $C_{\alpha r}$ represent the cornering stiffness of the front and rear tire, respectively. The slip angle of the front tire is α_f and is calculated as $\alpha_f = \delta - (\nu + l_f \omega)/v$. The rear tire slip angle is α_r and is calculated as $\alpha_r = (l_r \omega - \nu)/v$.

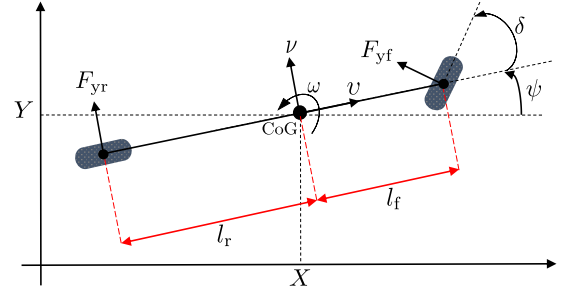


Fig. 1: Vehicle dynamics representation

TABLE I: Vehicle parameters

Symbol	Variables	Unit
X	Global X-axis coordinates of the vehicle's CoG	m
Y	Global Y-axis coordinates of the vehicle's CoG	m
v	Longitudinal velocity of the vehicle	m/s
ν	Lateral velocity of the vehicle	m/s
ψ	Yaw angle of the vehicle	rad
ω	Yaw rate of the vehicle	rad/s
δ	Steering angle of the front tire	rad
a	Longitudinal acceleration of the vehicle	m/s ²
α_f	Front tire slip angle	rad
α_r	Rear tire slip angle	rad
Symbol	Parameter	Value/Unit
$C_{\alpha f}$	Cornering stiffness front tire	156 kN/rad
$C_{\alpha r}$	Cornering stiffness rear tire	193 kN/rad
l_f	Distance CoG to front axle	1.04 m
l_r	Distance CoG to rear axle	1.4 m
I_z	Vehicle yaw inertia	2937 kgm ²
m	Vehicle mass	1919 kg

The parameters and variables are illustrated in Fig. 1 and in Table I.

To utilize the model in Eq. (3) in an MPC framework, it is necessary to discretize the model. One of the commonly used methods for obtaining the corresponding discrete-time system is the forward Euler method¹. Therefore, the vehicle dynamics in Eq. (3) can be written as in Eq. (1), where $z_k = [X_k \ Y_k \ v_k \ \nu_k \ \psi_k \ \omega_k]^T$, $u_k = [\delta_k \ a_k]^T$ with the sampling time given in Table II.

B. Constraints

To ensure the vehicle stays within the boundaries of the road, constraints are enforced on the (X_k, Y_k) coordinates of the vehicle. One approach [12], involves computing the lateral error of the vehicle's center of gravity, e_k^{lat} as follows

$$e_k^{\text{lat}} = -\sin(\psi_k^{\text{ref}})(X_k - X_k^{\text{ref}}) + \cos(\psi_k^{\text{ref}})(Y_k - Y_k^{\text{ref}}), \quad (4)$$

where X_k^{ref} , Y_k^{ref} and ψ_k^{ref} are the longitudinal position, the lateral position, and the orientation, respectively, on a point on a given reference trajectory at step k . Then, the following constraint ensures that the vehicle's CoG always stays within the boundaries of the road

$$-R_{1,k} \leq e_k^{\text{lat}} \leq R_{2,k}, \quad (5)$$

where $R_{1,k}$ and $R_{2,k}$ are the road widths on the right and left sides of the reference trajectory at step k . The

¹Forward Euler: $\dot{z}(t_k) \approx \frac{z(t_k + t_s) - z(t_k)}{t_s}$, for $t_k = t_s k$, $k = 0, 1, \dots$

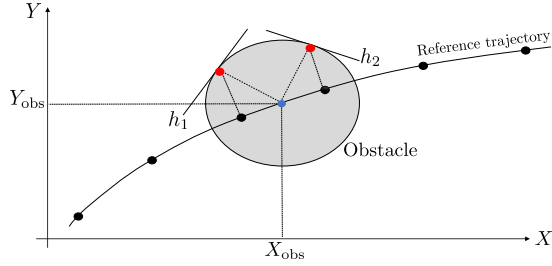


Fig. 2: Linear obstacle constraint computation. The center of the obstacle $(X_{\text{obs}}, Y_{\text{obs}})$ is marked by the blue dot, and the reference trajectory is represented by the solid line with black dots.

constraints associated with the road boundaries in Eq. (5) can be computationally expensive due to their nonlinear nature. To address this challenge, an alternative linear constraint is proposed as follows

$$\begin{bmatrix} a_{1,k} & b_{1,k} \\ -a_{2,k} & -b_{2,k} \end{bmatrix} \begin{bmatrix} X_k \\ Y_k \end{bmatrix} \leq \begin{bmatrix} c_{1,k} \\ -c_{2,k} \end{bmatrix}, \quad (6)$$

where $-a_{1,k}X_k - b_{1,k}Y_k \geq -c_{1,k}$ and $a_{2,k}X_k + b_{2,k}Y_k \geq c_{2,k}$ are half-spaces defined by the tangent to the road boundary at step k , which ensure the (X_k, Y_k) coordinates at step k to remain within the two half-spaces. Imposing such linear constraints allows more efficient computations in the MPC optimization problem.

An efficient representation of an obstacle is to be formulated as an ellipse. For simplicity, we consider here circular obstacles. To impose the obstacle constraints in the NMPC, one possible approach is to calculate the Euclidean distance between the (X_k, Y_k) coordinates and the center of the obstacle and to ensure that the vehicle's (X_k, Y_k) coordinates always remain outside the obstacle, as described below

$$(X_{\text{obs}} - X_k)^2 + (Y_{\text{obs}} - Y_k)^2 \geq r^2, \quad (7)$$

where $(X_{\text{obs}}, Y_{\text{obs}})$ indicates the center of the obstacle and r represents its radius. However, it is usually desired to formulate linear constraints for the obstacle in order to reduce the computational complexity. For this purpose, we propose to replace the nonlinear constraint in Eq. (7) with a linear inequality constraint, see Eq. (8) below, which varies over the MPC prediction horizon according to the tangent to the circular obstacle boundary. Every linear inequality constraint represents a half-space, which defines a safe region to avoid collision with the obstacle. An illustration is depicted in Fig. 2. If a reference point falls inside the obstacle within the MPC horizon, a tangent defining a linear inequality constraint, such as h_1 or h_2 , is calculated at the intersection point (the red dots in Fig. 2). The corresponding half-space includes the safe region to avoid the obstacle. The (X_k, Y_k) coordinate of the vehicle should then be on that side, which can be defined by the linear inequality

$$h_1 : a_{3,k}X_k + b_{3,k}Y_k \geq c_{3,k}, \quad (8)$$

where $a_{3,k}$, $b_{3,k}$ and $c_{3,k}$ are the parameters of the tangent half-space to the obstacle.

III. CONTROLLER DESIGN

A. The Kinematic Trajectories From a Fixed Map

To consider a realistic setup for the problem, we assume that only the $(X_i^{\text{ref}}, Y_i^{\text{ref}})$ values of the reference trajectory are available. However, we should compute the corresponding reference values for the remaining four states, $v_k^{\text{ref}}, \nu_k^{\text{ref}}, \psi_k^{\text{ref}}$ and ω_k^{ref} , to track the reference trajectory effectively. For the computation of ψ_k^{ref} , the global $(X_i^{\text{ref}}, Y_i^{\text{ref}})$ can be directly used as follows

$$\psi_k^{\text{ref}} = \arctan \left(\frac{Y_{k-1}^{\text{ref}} - Y_k^{\text{ref}}}{X_{k-1}^{\text{ref}} - X_k^{\text{ref}}} \right). \quad (9)$$

Next, ω_k^{ref} can be calculated as $\omega_k^{\text{ref}} = (\psi_k^{\text{ref}} - \psi_{k-1}^{\text{ref}})/t_s$, where ψ_{k-1}^{ref} is the reference yaw angle which was computed in the previous step by using Eq. (9). To calculate v_k^{ref} and ν_k^{ref} , which represent the longitudinal and lateral speeds in the body frame, the reference points in the body frame are determined as follows

$$\begin{bmatrix} x_k^{\text{ref}} \\ y_k^{\text{ref}} \end{bmatrix} = \begin{bmatrix} \cos(\psi_k^{\text{ref}}) & \sin(\psi_k^{\text{ref}}) \\ -\sin(\psi_k^{\text{ref}}) & \cos(\psi_k^{\text{ref}}) \end{bmatrix} \begin{bmatrix} X_k^{\text{ref}} - X_{k-1}^{\text{ref}} \\ Y_k^{\text{ref}} - Y_{k-1}^{\text{ref}} \end{bmatrix}. \quad (10)$$

Then, the reference speeds can be readily computed as $v_k^{\text{ref}} = (x_k^{\text{ref}} - x_{k-1}^{\text{ref}})/t_s$ and $\nu_k^{\text{ref}} = (y_k^{\text{ref}} - y_{k-1}^{\text{ref}})/t_s$, where x_i^{ref} and y_i^{ref} are computed in Eq. (10).

B. Nonlinear MPC

The constrained nonlinear optimal control for reference tracking w.r.t the decision variable $U = \{u_{0|k}, u_{1|k}, \dots, u_{N-1|k}\}$ is formulated as follows.

Problem 1 (Nonlinear optimization problem):

$$\min_U \|z_{N|k} - z_{N|k}^{\text{ref}}\|_P^2 + \sum_{i=0}^{N-1} \|z_{i|k} - z_{i|k}^{\text{ref}}\|_Q^2 + \|u_{i|k}\|_R^2 \quad (11a)$$

$$\text{s.t. } z_{i+1|k} = z_{i|k} + t_s f(z_{i|k}, u_{i|k}), \forall i = 0, \dots, N-1, \quad (11b)$$

$$z_{0|k} = z_k, \quad (11c)$$

$$z_{i|k} \in \mathcal{Z}_{i|k}, \quad \forall i = 0, 1, \dots, N, \quad (11d)$$

$$u_{i|k} \in \mathcal{U}, \quad \forall i = 0, 1, \dots, N-1, \quad (11e)$$

where $z_{i|k}^{\text{ref}} = [X_{i|k}^{\text{ref}} \ Y_{i|k}^{\text{ref}} \ v_{i|k}^{\text{ref}} \ \nu_{i|k}^{\text{ref}} \ \psi_{i|k}^{\text{ref}} \ \omega_{i|k}^{\text{ref}}]^\top$ is the reference value for the states at each step, which is computed by Eqs. (9) and (10). The tuning matrices are $Q \succeq 0 \in \mathbb{R}^{6 \times 6}$, $R \succ 0 \in \mathbb{R}^{2 \times 2}$ and $P \succeq 0 \in \mathbb{R}^{6 \times 6}$. The MPC prediction horizon is denoted with N . In the above optimization problem, f is the nonlinear dynamic bicycle model in Eq. (3), and $z_{0|k}$ is the system's initial condition. Here state constraint, $\mathcal{Z}_{i|k}$, includes the bounds on each state, the road boundary constraint (6), and the obstacle avoidance constraint (7). The input constraint \mathcal{U} is defined in Eq. (2).

C. Linear Parameter Varying MPC

By introducing the scheduling signals $v(t)$, $\nu(t)$, $\delta(t)$, and $\psi(t)$, that form the scheduling variable vector $p(t) =$

$(v(t), \nu(t), \delta(t), \psi(t))$; the continuous-time nonlinear dynamics in Eq. (3) can be written equivalently in the LPV representation as

$$\begin{cases} \dot{z}(t) = A_c(p(t))z(t) + B_c(p(t))u(t), \\ p(t) = (v(t), \nu(t), \delta(t), \psi(t)), t \geq 0. \end{cases} \quad (12)$$

The state vector $z(t)$ of dimension 6 can be defined as $z(t) := [X(t) \ Y(t) \ v(t) \ \nu(t) \ \psi(t) \ \omega(t)]^\top$ with initial conditions z_0 and the continuous-time system matrices $A_c \in \mathbb{R}^{6 \times 6}$, $B_c \in \mathbb{R}^{2 \times 2}$ as

$$A_c(p(t)) := \begin{bmatrix} 0 & 0 & \cos(\psi(t)) & -\sin(\psi(t)) & 0 & 0 \\ 0 & 0 & \sin(\psi(t)) & +\cos(\psi(t)) & 0 & 0 \\ 0 & 0 & 0 & 0 & 0 & \nu(t) \\ 0 & 0 & 0 & a_{44}(t) & 0 & a_{46}(t) \\ 0 & 0 & 0 & 0 & 0 & 1 \\ 0 & 0 & 0 & a_{64}(t) & 0 & a_{66}(t) \end{bmatrix},$$

$$\beta_f := \frac{2Caf}{m}, \beta_r := \frac{2Car}{m}, \gamma_f := \frac{2\ell_f C_{af}}{I_z}, \gamma_r := \frac{2\ell_r C_{ar}}{I_z},$$

$$a_{44}(t) := -\beta_f \cos(\delta(t)) \frac{1}{v(t)} - \beta_r \frac{1}{v(t)},$$

$$a_{46}(t) := -v(t) - \beta_f \cos(\delta(t)) \frac{1}{v(t)} \ell_f + \beta_r \frac{1}{v(t)} \ell_r,$$

$$a_{64}(t) := \frac{1}{v(t)} (\gamma_r - \gamma_f), \quad a_{66}(t) := -\frac{1}{v(t)} (\gamma_f \ell_f + \gamma_r \ell_r),$$

and

$$B_c(p(t)) := \begin{bmatrix} 0 & 0 & 0 & \beta_f \cos(\delta(t)) & 0 & \gamma_f \\ 0 & 0 & 1 & 0 & 0 & 0 \end{bmatrix}^\top.$$

The discretization with the Euler method and a sampling time t_s results in the discrete-time LPV representation of Eq. (12) as

$$\begin{cases} z_{k+1} = A(p_k)z_k + B(p_k)u_k, \\ p_k = (v_k, \nu_k, \delta_k, \psi_k), k \in \mathbb{Z}_+ \cup \{0\} \end{cases} \quad (13)$$

where $A(p_k) = I + t_s A_c(p_k)$, $B(p_k) = t_s B_c(p_k)$ are the discrete-time LPV system matrices, and $I \in \mathbb{R}^{6 \times 6}$ is the identity matrix.

Problem 2: QP optimization as $\text{QP}(p_{i|k}, z_k, z_{i|k}^{\text{ref}})$

$$\min_U \|z_{N|k} - z_{N|k}^{\text{ref}}\|_P^2 + \sum_{i=0}^{N-1} \|z_{i|k} - z_{i|k}^{\text{ref}}\|_Q^2 + \|u_{i|k}\|_R^2 \quad (14a)$$

$$\text{s.t. } z_{i+1|k} = A(p_{i|k})z_{i|k} + B(p_{i|k})u_{i|k}, \quad i = 0, \dots, N-1 \quad (14b)$$

$$z_{0|k} = z_k, \quad (14c)$$

$$z_{i|k} \in \bar{\mathcal{Z}}_{i|k}, \quad \forall i = 0, 1, \dots, N, \quad (14d)$$

$$u_{i|k} \in \mathcal{U}, \quad \forall i = 0, 1, \dots, N-1, \quad (14e)$$

where, the reference trajectory $z_{i|k}^{\text{ref}}$, the tuning matrices P , Q and R , as well as the decision variable U are as defined for the Problem 1. The initial condition is $z_{0|k}$, and N denotes the MPC prediction horizon. The LPV model in Eq. (14b) is defined in Eq. (13). The input constraint \mathcal{U} is given in Eq. (2). The state constraint $\bar{\mathcal{Z}}_{i|k}$ in Eq. (14d) includes the bounds on the states, the road boundary constraint in Eq. (6) and the linear obstacle avoidance constraint in Eq. (8). Therefore, the state constraint can be represented in the polytopic form $\bar{\mathcal{Z}}_k = \{z_k \in \mathbb{R}^6 | G_k^z z_k \leq h_k^z\}$. The steps implementing the above LPVMPC are given in Algorithm 1. A similar algorithm has been proposed for the quasi LPV case in [13].

Algorithm 1 The QP-based LPVMPC algorithm

Input: Initial conditions z_k , and the road reference (X_k, Y_k) , $k \in \mathbb{Z}_+$.

Output: The control input u_k , $k = 1, \dots$, that drives the nonlinear system to the reference while avoiding obstacles.

1: Initialize for $k = 0$ the scheduling vector $\hat{p}_{i|0}$ as

$$\hat{p}_{i|0} := (v_0, \nu_0, \delta_0, \psi_0), \quad i = 0, \dots, N-1$$

2: **while** $k = 0, 1, \dots$ **do**

3: Update the state $z_{i|k}^{\text{ref}}$ as explained in Section III-A.

4: Solve the QP in Problem 2

$$[z_{i+1|k}, u_{i|k}] \leftarrow \text{QP}(\hat{p}_{i|k}, z_k, z_{i|k}^{\text{ref}}), \quad i = 0, \dots, N-1$$

$$\text{Update } \hat{p}_{i|k} := (\hat{v}_{i|k}, \hat{\nu}_{i|k}, u_{i|k}, \hat{\psi}_{i|k}), \quad i = 0, \dots, N$$

5: Apply $u_k = u_{0|k}$ to the system

6: Measure z_{k+1}

7: Update $\hat{p}_{i|k+1} = \hat{p}_{i+1|k}$, $i = 0, \dots, N-1$

8: $k \leftarrow k + 1$

9: **end while**

IV. RESULTS AND DISCUSSIONS

This section implements and compares the performance of the two MPCs, the NMPC and the LPVMPC. The simulations are performed on a Dell Latitude 5590 laptop with an Intel(R) Core(TM) i7-8650U CPU and 16 GB of RAM. The scenarios are implemented in Matlab [14], utilizing the YALMIP toolbox [15], with an optimality tolerance of 10^{-4} . To solve the nonlinear optimization problem, we employ the *IPOPT* solver [16]. The Matlab *quadprog* solver is used for solving the quadratic optimization problem.

The simulation scenario is to drive the vehicle in the middle on the right-hand side of a road to follow a reference trajectory using one of the proposed controllers in the previous sections. Then, an obstacle appears in the road, and the vehicle is controlled to overtake this obstacle safely and to return back to the reference trajectory in the middle on the right-hand side of the road. Table II presents the parameters utilized in the MPCs, along with the upper and lower limits of the states and input variables.

TABLE II: MPC Parameters

Parameter	Value	Parameter	Value
Lower bound on X_k	-1 m	Upper bound on X_k	150 m
Lower bound on Y_k	-1 m	Upper bound on Y_k	120 m
Lower bound on v_k	1 $\frac{\text{m}}{\text{s}}$	Upper bound on v_k	100 $\frac{\text{m}}{\text{s}}$
Upper bound on $ \nu_k $	10 $\frac{\text{m}}{\text{s}}$	Upper bound on $ \psi_k $	$\pi/2$ rad
Upper bound on $ \omega_k $	$\frac{\pi}{4t_s}$ $\frac{\text{rad}}{\text{s}}$	Sampling time t_s	0.05 s
Upper bound on $ \delta_k $	$\frac{34\pi}{180}$ rad	Sampling frequency f_s	20 Hz
Lower bound on a_k	-6 $\frac{\text{m}}{\text{s}^2}$	Upper bound on a_k	2 $\frac{\text{m}}{\text{s}^2}$

The reference trajectory is picked as a sine wave to mimic the road, and the $(X_i^{\text{ref}}, Y_i^{\text{ref}})$ on the reference trajectory are intentionally selected to be non-equidistant in space. As a result, the vehicle's speed shall be adjusted based on the distance between successive $(X_i^{\text{ref}}, Y_i^{\text{ref}})$ points. The initial condition of the vehicle is $z_0 = [0 \ 0 \ 10 \ 0 \ 0 \ 0]^\top$. Furthermore, the road on the left-hand side of the vehicle's

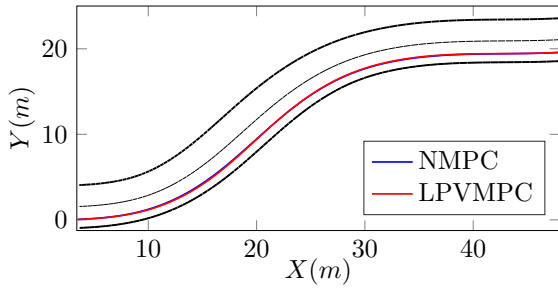


Fig. 3: Reference tracking by NMPC and LPVMPC

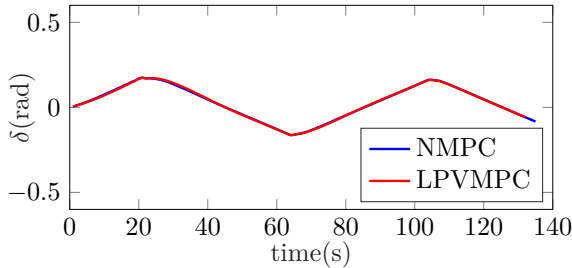


Fig. 4: Reference tracking steering angles by NMPC and LPVMPC

reference trajectory is assumed to be always 4 m wide, while on the right-hand side, it is always only 1 m wide, i.e., $R_{1,k} = 1$ m and $R_{2,k} = 4$ m, $\forall k = 0, 1, \dots$ in Eq. (5). Also, for both MPCs, $N = 8$, $R = \text{diag}([0.1 \ 0.1])$, $Q = \text{diag}([10 \ 10 \ 1 \ 1 \ 1 \ 1])$ and $P = Q$. To keep the vehicle movements smoother, we constrain the rate of change of δ_k and a_k , i.e., $|\delta_k - \delta_{k-1}| \leq 40\pi/180$ rad, $|a_k - a_{k-1}| \leq 1.5$ m/s².

To evaluate the effectiveness of our approach, we compare the performance of the NMPC and the LPVMPC in two problem setups: a reference tracking (RT) problem and an obstacle avoidance problem.

A. Reference Tracking (RT)

In Fig. 3, a comparison of the application of the NMPC and the LPVMPC for reference tracking is demonstrated. In this figure, the blue line represents the position of the vehicle when controlled by the NMPC, and the red line is the position of the vehicle controlled by the LPVMPC. As illustrated in Fig. 3, the performance of the LPVMPC and the NMPC regarding tracking error is almost identical. By comparing the inputs generated by the controllers in Figs. 4 and 5, it is clear that the steering angles produced by the NMPC and LPVMPC are nearly identical. Similarly, the accelerations are quite similar, although the NMPC acceleration appears to be smoother. Table III displays the computation time for solving an optimization problem to generate the inputs for the NMPC and the LPVMPC at each time instant k . The results confirm the reduction in the computation time by using the LPVMPC.

B. Obstacle Avoidance

In this subsection, the results of the comparison between the NMPC and the LPVMPC in an obstacle avoidance scenario are presented. The obstacle is assumed to be in a

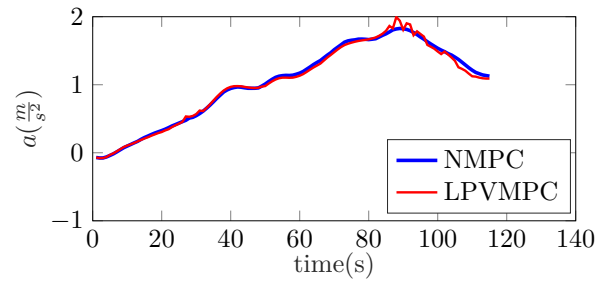


Fig. 5: Reference tracking accelerations by NMPC and LPVMPC

TABLE III: Comparison of computation times using YALMIP between NMPC and LPVMPC for a reference tracking scenario

RT w/o obstacle	NMPC	LPVMPC
Average time	0.2602 s	0.0067 s
Maximum time	1.4996 s	0.0848 s
Minimum time	0.0739 s	0.0037 s

circular shape with a radius of 1 m at $X_{\text{obs}} = 29.4819$ m, $Y_{\text{obs}} = 17.4753$ m. This means that the obstacle has blocked one side of the road in the studied scenario.

The result of applying each of these MPCs to the nonlinear vehicle dynamics Eq. (3) is illustrated in Fig. 6. In this figure, the blue line represents the vehicle's trajectory when controlled by the NMPC, while the red line indicates its trajectory when controlled by the LPVMPC. As Fig. 6 indicates, both the NMPC and LPVMPC are capable of controlling the vehicle to follow the desired reference trajectory and initiate the overtaking maneuver at an appropriate moment. However, the NMPC is performing a smoother maneuver. In Figs. 7 and 8, the steering angles and the accelerations generated by each controller are presented. Based on the information in these figures, the NMPC can generate smoother control inputs. The difference in the inputs justifies the smoother movement of the vehicle in Fig. 6. The computation time of both the NMPC and the LPVMPC are presented in Table IV. As the results confirm, using the LPVMPC can reduce the computation time significantly.

V. CONCLUSIONS

This paper proposed a novel LPV embedding for modeling the nonlinear dynamics of a vehicle with linear tire forces. The proposed approach aims to simplify the implementation and offers a good alternative to NMPC, which is commonly

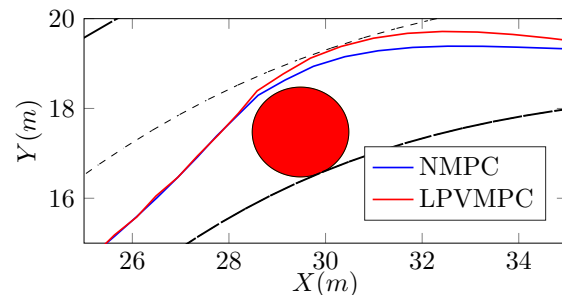


Fig. 6: Obstacle avoidance scenarios by NMPC and LPVMPC. The car overtakes the obstacle with a longitudinal speed of around 50 km/h.

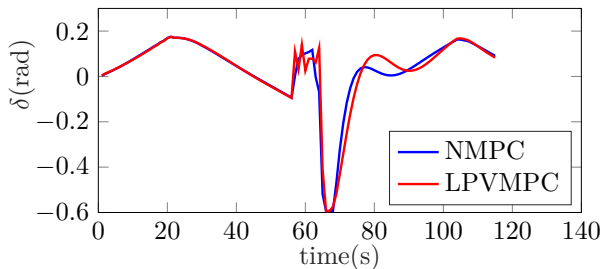


Fig. 7: Obstacle avoidance steering angles by NMPC and LPVMPC

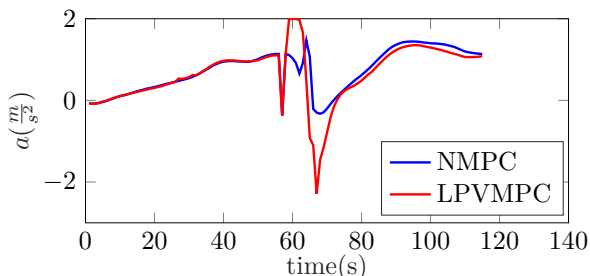


Fig. 8: Obstacle avoidance accelerations by NMPC and LPVMPC

TABLE IV: Comparison of computation times using YALMIP between NMPC and LPVMPC for an obstacle avoidance scenario

RT with obstacle	NMPC	LPVMPC
Average time	0.7187 s	0.0066 s
Maximum time	4.2031 s	0.0857 s
Minimum time	0.2559 s	0.0037 s

considered. We introduced a linear formulation for obstacle avoidance constraints, enabling the proposed LPVMPC scheme to integrate both path planning and control into a single optimization problem. The LPVMPC is comparable to the NMPC in terms of performance with a more efficient computational burden. Finally, better tuning, model generalizations with the LPV embedding, dynamical and more challenging obstacles avoidance scenarios, as well as considering theoretical analysis such as stability and recursive feasibility guarantees are left for future research endeavors as the analysis with the LPV formulation can be carried out efficiently within the well-defined linear systems framework.

REFERENCES

- [1] M. Nezami, G. Männel, H. S. Abbas, and G. Schildbach, "A safe control architecture based on a model predictive control supervisor for autonomous driving," in *2021 European Control Conference (ECC)*, IEEE, 2021, pp. 1297–1302.
- [2] M. Nezami, N. T. Nguyen, G. Männel, H. S. Abbas, and G. Schildbach, "A safe control architecture based on robust model predictive control for autonomous driving," in *2022 American Control Conference (ACC)*, IEEE, 2022, pp. 914–919.
- [3] T. Brüdigam, M. Olbrich, D. Wollherr, and M. Leibold, "Stochastic model predictive control with a safety guarantee for automated driving," *IEEE Transactions on Intelligent Vehicles*, 2021.
- [4] J. P. Allamaa, P. Listov, H. Van der Auweraer, C. Jones, and T. D. Son, "Real-time nonlinear MPC strategy with full vehicle validation for autonomous driving," in *2022 American Control Conference (ACC)*, IEEE, 2022, pp. 1982–1987.
- [5] J. Lee and S. Choi, "Nonlinear model predictive control for path tracking in high-speed corner entry situations," *International Journal of Automotive Technology*, vol. 23, no. 5, pp. 1373–1381, 2022.
- [6] S. Arrigoni, F. Braghin, and F. Cheli, "MPC trajectory planner for autonomous driving solved by genetic algorithm technique," *Vehicle system dynamics*, vol. 60, no. 12, pp. 4118–4143, 2022.
- [7] M. H. de Lange, C. Verhoek, V. Preda, and R. Tóth, "LPV modeling of the atmospheric flight dynamics of a generic parafoil return vehicle," *IFAC-PapersOnLine*, vol. 55, no. 35, pp. 37–42, 2022.
- [8] M. Bujarbaruah, U. Rosolia, Y. R. Stürz, X. Zhang, and F. Borrelli, "Robust MPC for LPV systems via a novel optimization-based constraint tightening," *Automatica*, vol. 143, p. 110459, 2022.
- [9] M. Nezami, H. S. Abbas, N. T. Nguyen, and G. Schildbach, "Robust tube-based LPV-MPC for autonomous lane keeping," *IFAC-PapersOnLine*, vol. 55, no. 35, pp. 103–108, 2022.
- [10] E. Alcalá, V. Puig, and J. Quevedo, "LPV-MP planning for autonomous racing vehicles considering obstacles," *Robotics and Autonomous Systems*, vol. 124, p. 103392, 2020.
- [11] R. Rajamani, *Vehicle dynamics and control*. Springer Science & Business Media, 2011.
- [12] B. Tearle, K. P. Wabersich, A. Carron, and M. N. Zeilinger, "A predictive safety filter for learning-based racing control," *IEEE Robotics and Automation Letters*, vol. 6, no. 4, pp. 7635–7642, 2021.
- [13] P. S. G. Cisneros, S. Voss, and H. Werner, "Efficient nonlinear model predictive control via quasi-LPV representation," in *2016 IEEE 55th Conference on Decision and Control (CDC)*, 2016, pp. 3216–3221.
- [14] MATLAB, *Vehicle Dynamics Blockset. Version 1.2 (R2019a)*. Natick, Massachusetts, United States: The MathWorks Inc., 2019.
- [15] J. Löfberg, "YALMIP : A toolbox for modeling and optimization in matlab," in *In Proceedings of the CACSD Conference*, Taipei, Taiwan, 2004.
- [16] A. Wächter and L. T. Biegler, "On the implementation of an interior-point filter line-search algorithm for large-scale nonlinear programming," *Mathematical programming*, vol. 106, pp. 25–57, 2006.